

GWO-PID of Two-Phase Hybrid Stepping Motor for Robotic Grinding Force

Fatin Nabeel Abdullah¹, Ghada Adel Aziz² Salam Waley Shneen^{3,*}
^{1,2,3} University of Technology - Iraq, Baghdad, Iraq

Email: ¹ 50060@uotechnology.edu.iq, ² 50070@uotechnology.edu.iq, ³ salam.w.shneen@uotechnology.edu.iq

*Corresponding Author

Abstract—The use of the computer program MATLAB is prominent in many studies that simulate many industrial systems. The current simulation aims to build a suitable simulation model representing the Two-phase Hybrid Stepping Motor (2Ph-HSM). This type of motor is employed in a specific application to produce a force called automatic grinding force. To control the force, motor speed, and location, we need to add control systems, so two methods have been proposed, one of which is traditional, namely proportional, integral, and derivative (PID) control and the other is intelligent, called Gray Wolf Optimization (GWO). The current work also aims to use traditional control algorithms and advanced optimization algorithms that were chosen for their ease of control and possibility of use in many industrial applications. By setting appropriate specifications for the simulation model and after conducting prescribed tests that simulate different applications of the motor's work within electrical systems, the results demonstrated good motor performance, better response, and high accuracy, in addition to speed. The goal is to design and tune a proportional, integral, and derivative (PID) controller by gray wolf optimization (GWO) using the transfer function (TF) of a 2Ph-HSM. To adjust the parameters of conventional controllers using advanced optimization, a suitable mechanism and technique were selected from advanced optimization techniques, where the gray wolf technique algorithm was chosen as an optimization technique and Integrated Time Absolute Error (ITAE) to adjust the parameters of conventional PID controller.

Keywords— GWO-PID; PID; RGS; 2Ph-HSM

I. INTRODUCTION

Previous studies confirmed the possibility of using computer programs, including the MATLAB engineering program, to simulate systems that focus on operating electric motors in various fields. Previous studies have also confirmed the possibility of representing electric motors with mathematical models and block diagrams [1]-[5]. The conversion function of the system can be calculated according to the appropriate specifications. The 2Ph-HSM motor is one of the motors that has gained a great deal of importance in industrial applications, including moving and rotating a robot arm in the grinding process of curved surfaces such as a fan. The ship is the subject of current simulations [6]-[10].

Electric motors need control units to improve their performance. Among the commonly used control units that have proven their efficiency with linear systems is the traditional controller [11]-[15]. While nonlinear systems need expert units such as neural networks and fuzzy logic or smart ones such as the optimal advance of a genetic algorithm or types. The work environment is considered to be on a turbine

blade or a marine fan that needs an environment suitable for constant force. The grinding process bends with the change of time. The workpiece bends on the work piece. We need to provide the required natural path for the grinding process accurately because of changing its dimensions during the grinding process and changing the dimensions as a result of the erosion of the piece by the impact of the grinding process [16]-[19].

The hierarchical wolf algorithm is one of the most important algorithms that previous experiments have demonstrated the possibility of using to improve the performance of linear and nonlinear systems. Among the categories that it includes is the leader and it is called alpha (α), which is considered the highest in the hierarchy or from the first level. The leader category is the one that cares and is able to make decisions, including choosing the spatial environment for hunting and the place to live. It does not matter if the leader is female, male, or both. Another category is beta (β), which is from the second level of the hierarchy, and this category assists the first category in making some decisions. There is also a third category, Delta (δ), and it is the lowest level in terms of hierarchy, and it is the category that is subject to orders. All categories are in the form of groups, and each has a role to play or what is called a scapegoat [20]-[24]. Finally, the Omega category (ω), which is the lowest category of the pyramid, or the fourth rank is called the category of sheiks, and its function is detection and guarding. All classes in the algorithm hierarchy can be represented by a flowchart of the wolves' algorithm as in the Fig. 1. Whereas Fig. 2 show the flow process of the method.

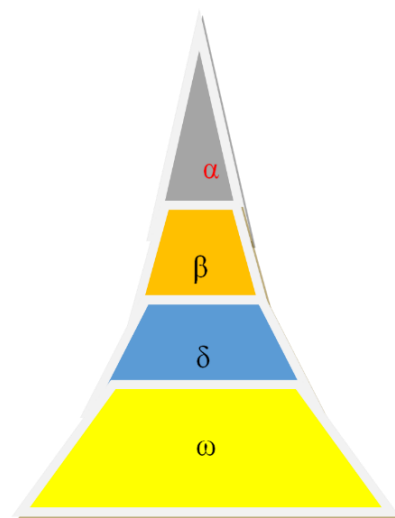


Fig. 1. Hierarchical wolf algorithm

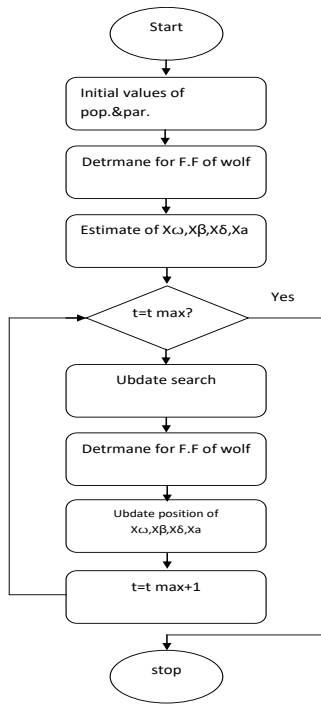


Fig. 2. Flow chart of hierarchical wolf algorithm

Performance indicators of the error in the system are the problem and its solution is to get rid of it completely or reduce it to the lowest possible level, thus obtaining an effective system design within the required outputs. The amount of error is taken and treated with one of the techniques of system performance indicators such as IAE, which means absolute integration of error [25]-[29]. There are other types that will be mentioned and represented in the equations (1-4) and Fig. 3, Fig. 4, Fig. 5, Fig. 6.

$$ISE = \int e^2(t)dt \tag{1}$$

$$IAE = \int |e(t)|dt \tag{2}$$

$$ITAE = \int t|e(t)|dt \tag{3}$$

$$ISTAE = \int t^2|e(t)|dt \tag{4}$$

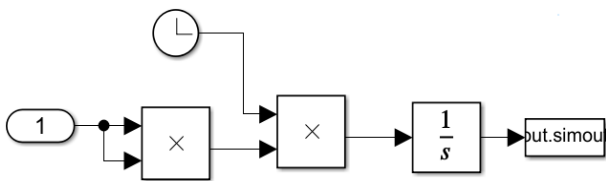


Fig. 3. Diagram of the ISE performance improvement index

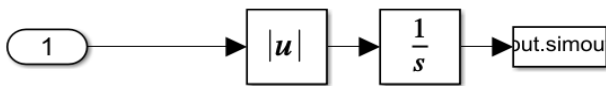


Fig. 4. Diagram of the IAE performance improvement index

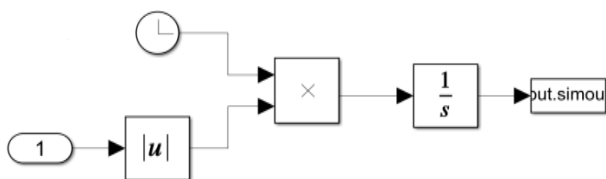


Fig. 5. Diagram of the ITAE performance improvement index

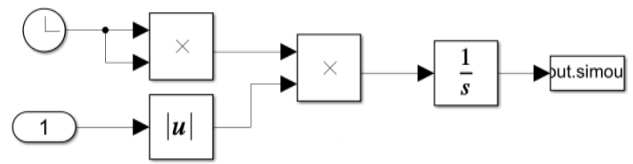


Fig. 6. Diagram of the ISTAE performance improvement index

To obtain an effective and appropriate system response, an objective function of the type ITAE was chosen. It means the integration of the absolute error multiplied by time. It is based on the measurement of the error value during operation $e(t)$ and is calculated from the difference between the actual speed (feedback) and the reference (required). It can be mathematically represented by an equation and as a model [30]-[34].

After representing the model mathematically and arriving at a transfer function model that fits its specifications, the proposed tests were performed. The simulation results showed the possibility of representing and simulating the system in addition to the possibility of improving performance for the various proposed cases. In this simulation, we propose to test the possibility of representing the robotic arm, which is driven using an electric motor, to perform the milling process of a curved surface of the ship's hull from under the water, which requires a balanced effort and force to perform the work with high accuracy and proficiency. Therefore, this requires that all operating conditions be considered according to a suitable controller's business strategy and algorithm for its real-time operation [35]-[39].

The model can be represented mathematically and appropriate tests can be performed to simulate real-time operation. Three tests were developed for the purpose of comparison and to determine the importance of each condition and the negatives and positives through the simulation results of response speed, ascent, overtaking, stability, transient condition, and all associated working conditions. Improving work performance by adopting intelligent control systems that are compatible with the non-linear system, since the traditional control unit is only suitable for linear systems [40]-[44].

II. THE 2PH-HSM IN THE AUTOMATED MILLING PROCESS (RGS)

The grinding process is a mechanical process provided by the electric motor. The grinding process takes place as a result of the presence of materials to be removed from the surfaces of the required workpieces. The 2ph-HSM motor is used in the milling process as a result of its suitable torque as well as being suitable in terms of noise, vibration, and cost. The milling machine can be seen in Fig. 7, where there are clear forces for the milling process, normal, and tangential which are symbolized by f_N , f_T , and F_d . Fig. 8 represents the scheme of the system, which can be mathematically represented by the equations (5-8) [45]-[50].

After examining the components of the system and representing them mathematically, the next step is to build the simulation model in successive steps. Where: Tangential force is f_T , elastic modulus of a Helix Spring is K_f , smallest

displacement to compress the Helix Spring is ds , greatest displacement is dg , precise displacement is dp .

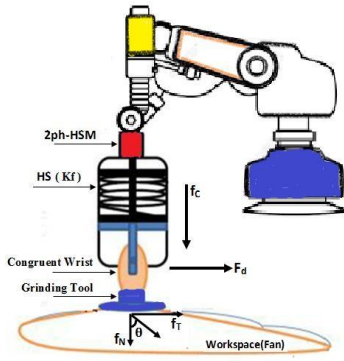


Fig. 7. Equivalents RGFS with hybrid stepper motor

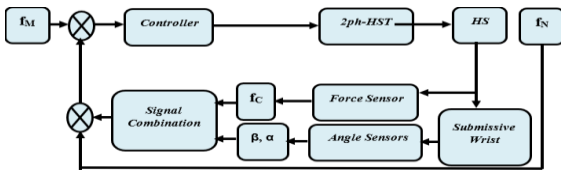


Fig. 8. Schematic diagram of RGFS with hybrid stepper motor

$$\rho = \tan \theta \quad (5)$$

$$f_T = \rho f_N \quad (6)$$

$$f_N = \frac{Kf(dg+ds)}{2} \quad (7)$$

$$d_p = \frac{dg+ds}{2} \quad (8)$$

The simulation model can be represented by an equivalent circuit and the appropriate transfer function. It represents the electrical circuit of the motor as in Fig. 9 and the transfer function is in (9).

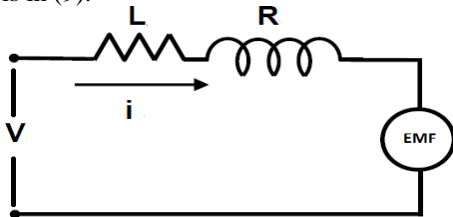


Fig. 9. Equivalent circuit for 2Ph-HSM

$$G(s) = \frac{A(s)}{B1(s) + B2(s)} \quad (9)$$

$$A(s) = Kpv + KIv / s + KDv s \quad (KPi s + KIi) ke NKH$$

$$B1(s) = J L s^4 + (JR + \beta L + JKPi KH) s^3$$

$$B2(s) = \beta KIi KH s + (JKIi KH + \beta R + \beta KPi KH) s^2$$

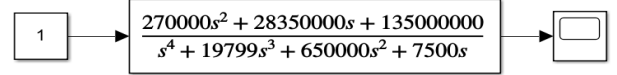
When the system specifications are known, the required transfer function for the simulation model can be written. The system specifications and the transfer function are as follows: Resistance $R = 1.3\Omega$, Inductance $L = 4.5mH$, Coefficient of Viscous Friction $B = 0 \text{ N}\cdot\text{m}\cdot\text{s}/\text{rad}$, Inertia Constant $J = 270 \text{ kg}\cdot\text{m}$, $\beta = 1$, $KDv = 115$, $Kpv = 550$, $KIi = 550$, $KIv = 0$, $ke = 0.25 \text{ N}\cdot\text{m}/\text{A}$, $KH = 10$, $KPi = 6$ and $N = 180$. Transfer function (TF) will be (10).

$$G(s) = \frac{270000 s^2 + 28350000 s + 135000000}{s^4 + 19799 s^3 + 650000 s^2 + 7500 s} \quad (10)$$

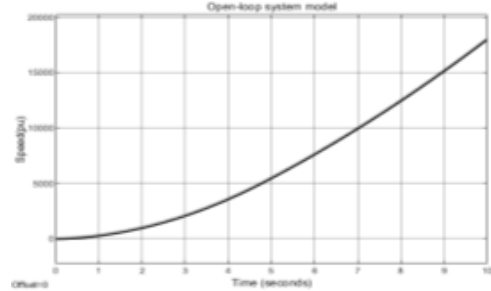
III. RESULTS AND DESCUSION

A. Open-loop system model

The behavior of the open-loop system can be studied in both linear and nonlinear systems using model and simulation results. For example, the reference value of the system is speed, and when the system operates with a fixed reference value of speed, this type is considered a linear system that can represent the simulation model as in Fig. 10 (a). The behavior of the system can be known through the simulation results as in Fig. 10 (b) while the non-linear system, which is when the system operates with a variable speed reference value, can represent the simulation model as in Fig. 11 (a) and the behavior of the system can be known through the simulation results as in Fig. 11 (b). From the figure, we notice the instability of the system is clear. This requires finding a solution for the stability of the system. It is suggested to build a closed-loop system and conduct a test to know the behavior of the system.

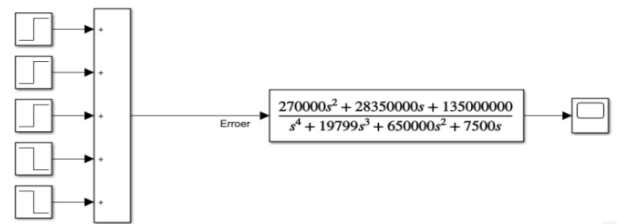


a. Simulation model

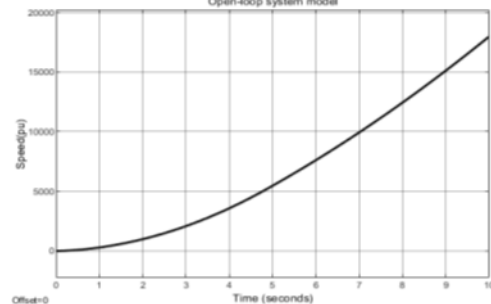


b. Simulation result

Fig. 10. Open-loop system model of a constant speed reference value



a. Simulation model

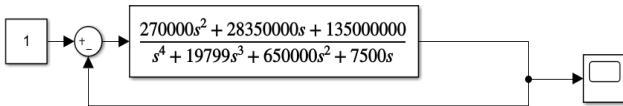


b. Simulation result

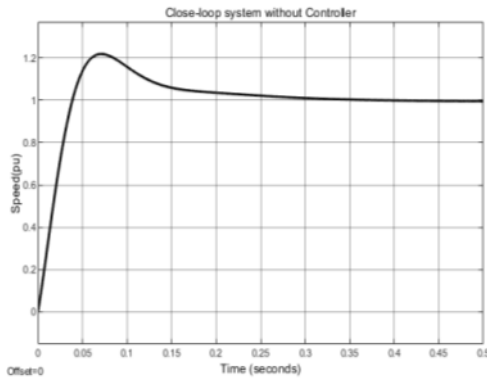
Fig. 11. Open-loop system of a variable speed reference value

B. Closed-loop system model

The behavior of the closed-loop system without a controller can be studied in both linear and nonlinear systems using model and simulation results. For example, the reference value of the system is speed, and when the system operates with a fixed reference value of speed, this type is considered a linear system that can represent the simulation model as in Fig. 12 (a). The behavior of the system can be known through the simulation results as in Fig. 12 (b), while the non-linear system, which is when the system operates with a variable speed reference value, can represent the simulation model as in Fig. 13 (a) and the behavior of the system can be known through the simulation results as in Fig. 13 (b).



a. simulation model without controller

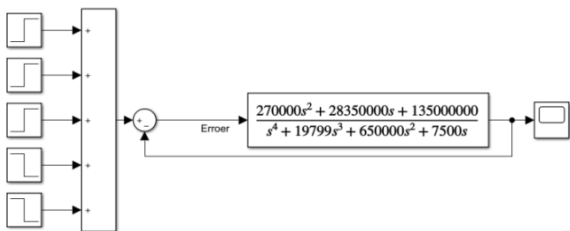


b. Simulation result without controller

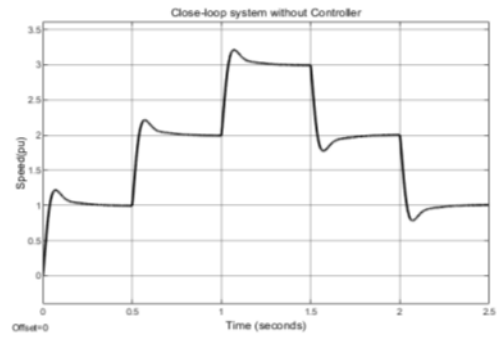
Fig. 12. close-loop system model of a constant speed reference value

The simulation model in Fig. 12 shows the conversion function with the reference signal and the oscilloscope for the (actual) output signal. We also note the presence of feedback, as well as a comparator between the reference and actual value, and the output of the comparator represents the error value. Fig. 13 represents the output of the oscilloscope and represents the closed-loop system behavior.

From the figure, we notice the transient state and the stable state by exceeding the output from the established limit, and then it returns to the required value. This requires finding a solution for the stability of the system while reducing the rate of overshoot and speed of performance. It is suggested to build a closed loop system with a conventional control unit and conduct the test to know the behavior of the system.



a. simulation model without controller

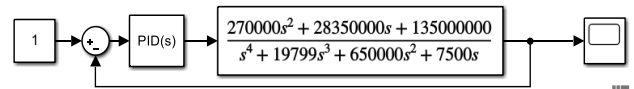


b. Simulation result without controller

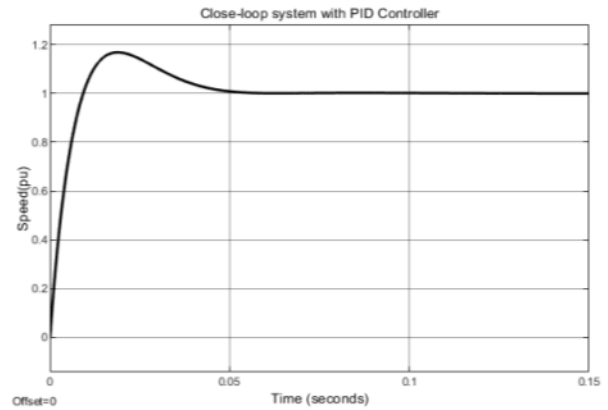
Fig. 13. close -loop system of a variable speed reference value

C. Closed loop system model with PID controller

The behavior of the closed-loop system with PID controller can be studied in both linear and nonlinear systems using model and simulation results. For example, the reference value of the system is speed, and when the system operates with a fixed reference value of speed, this type is considered a linear system that can represent the simulation model as in Fig. 14 (a). The behavior of the system can be known through the simulation results as in Fig. 14 (b), while the non-linear system, which is when the system operates with a variable speed reference value, can represent the simulation model as in Fig. 15 (a) and the behavior of the system can be known through the simulation results as in Fig. 15 (b).

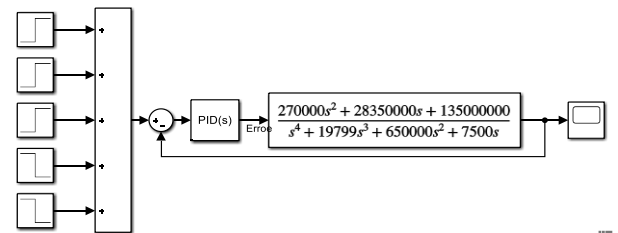


a. simulation model with PID controller

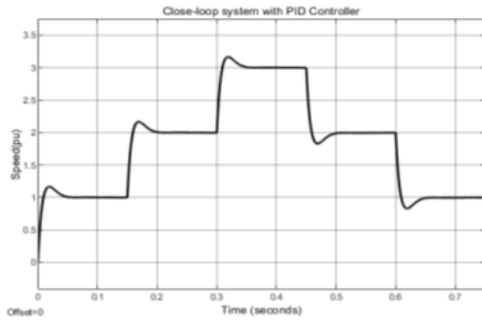


b. simulation results with PID controller

Fig. 14. close-loop system model of a constant speed reference value

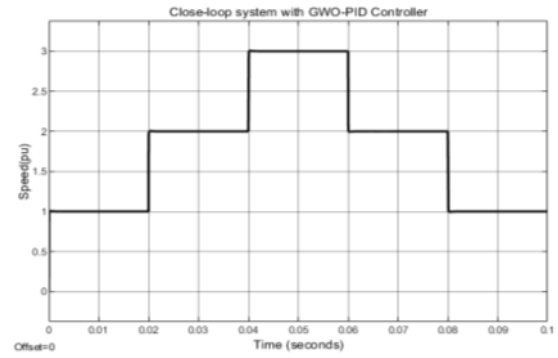


a. simulation model with PID controller



b. Simulation results with PID controller

Fig. 15. Close-loop system model of a variable speed reference value

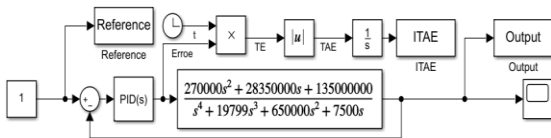


b. Simulation results with GWO-PID controller

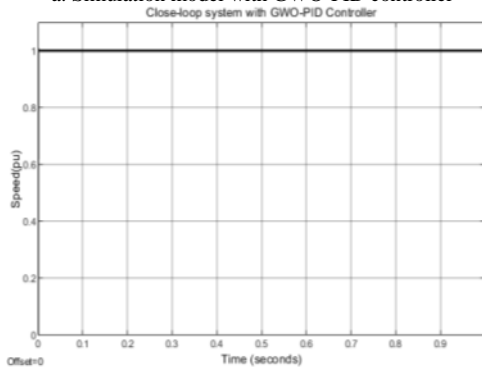
Fig. 17. Close-loop system model of a variable speed reference value

D. Closed loop system model with GWO-PID controller

The behavior of the closed-loop system with GWO-PID controller can be studied in both linear and nonlinear systems using model and simulation results. For example, the reference value of the system is speed, and when the system operates with a constant reference value of speed, this type is considered a linear system that can represent the simulation model as in Fig. 16 (a). The behavior of the system can be known through the simulation results as in Fig. 16 (b), while the non-linear system, which is when the system operates with a variable speed reference value, can represent the simulation model as in Fig. 17 (a) and the behavior of the system can be known through the simulation results as in Fig. 17 (b). Performance using the ITAE objective function with GWO-PID controller is shown in Fig. 18. The results can be appended in one form to show the difference between the different methods and to identify the best among them, as in Fig. 19.

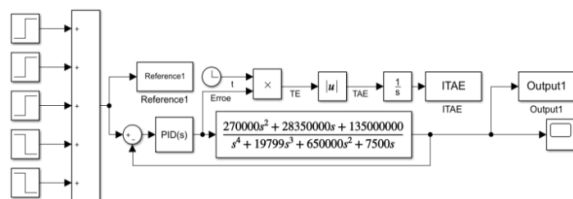


a. Simulation model with GWO-PID controller



b. Simulation results with GWO-PID controller

Fig. 16. Close-loop system model of a constant speed reference value



a. Simulation model with GWO-PID controller

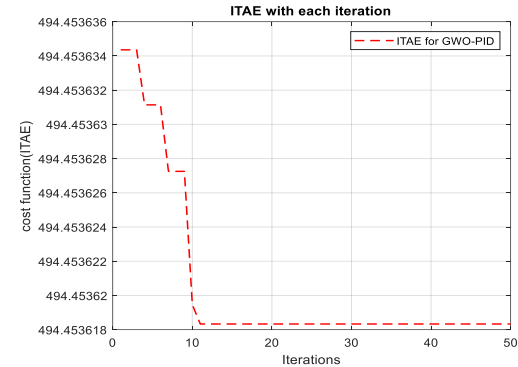


Fig. 18. Performance ITAE each iteration for GWO-PID controller

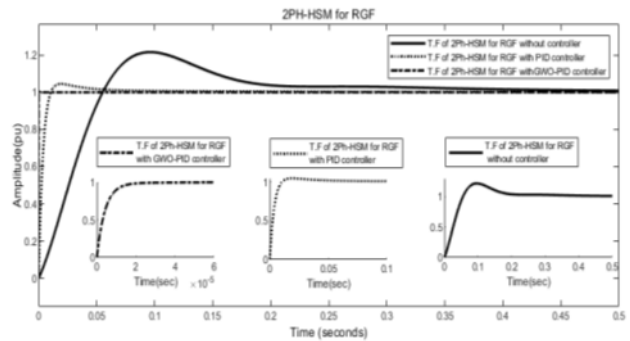


Fig. 19. Results of SM without, with PID and GWO-PID

To discuss the simulation results, we need to describe the behavior of the system for the proposed cases and adopt the comparison between the different tests. The measurement criteria are time, such as the rise time, the settling time, and the average rate of deviations from the desired goal. The fastest method is considered the best, and the least deviation rate characterizes the best method. The fastest way is by using the gray wolf algorithm and the lowest bypass rate was by the wolf algorithm.

In the simulation results section, there are three parts, The first part simulation model, under title modeling without a controller which means a close loop at the linear system, and the result of this model is shown in Fig. 20. Fig. 20 shows the rise time equal 42.7 ms, overshoot of 18.452%, and undershoot 2%. The second part, the simulation model under title modeling with PID controller at the close loop at liner system and the result of this model is shown in Fig. 21. Fig. 21 shows the rise time equal 6.603ms, overshoot amplitude equal 4.737% and undershoot 2%. Finally, part, simulation

model, under title modeling with GWO-PID controller means a close loop at the liner system, and the result of this model is shown in Fig. 22. Fig. 22 shows the rise time equal to 9.571ms, overshoot of -0.225%, undershoot of 1.980%, and settling time equal to 15.437 ms.

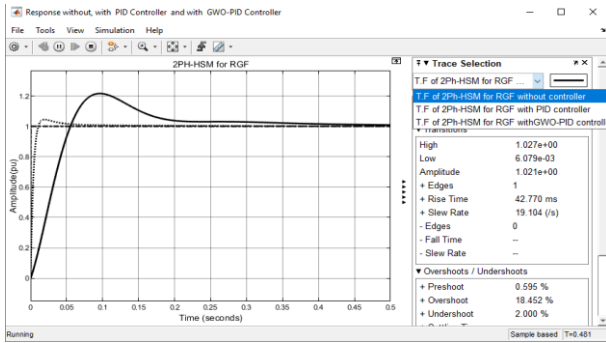


Fig. 20. Data results of first part

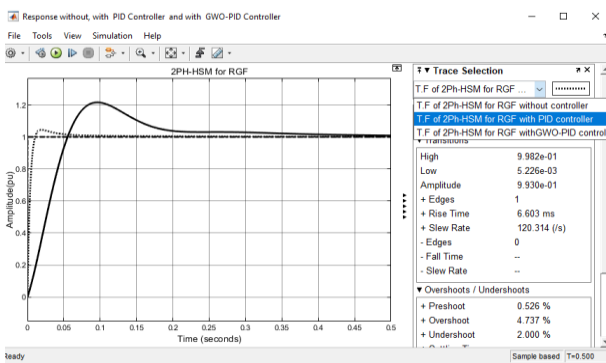


Fig. 21. Data result of second part

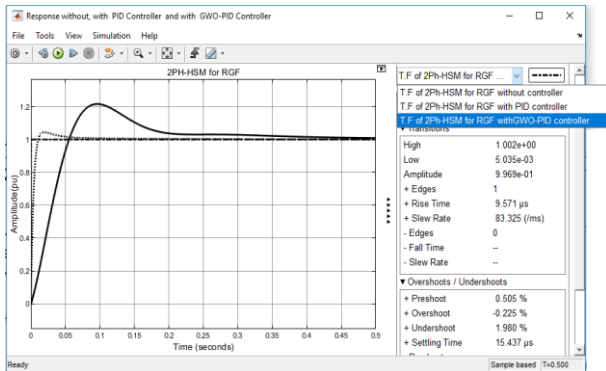


Fig. 22. Data of third part

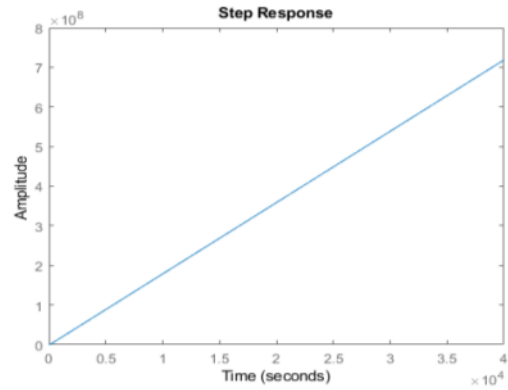
E. Modeling by m-file code

Another method of simulation can be presented by writing code that represents the system in the form of m-files, as in the forms of simulation models and simulation results in the following forms: First, open loop system, the modeling m-file as shown in Fig. 23 (a) and the simulation result as shown in Fig. 23 (b). Second, the close loop system without a controller, the modeling m-file as shown in Fig. 24 (a), and the simulation result as shown in Fig. 24 (b). Third, the close loop system with PID controller, the modeling m-file as shown in Fig. 25 (a), and the simulation result as shown in Fig. 25 (b). Fourth, the close loop system with GWO-PID controller, the modeling m-file as shown in Fig. 26 (a), and the simulation result as shown in Fig. 26 (b).

```

Editor - C:\Users\Lenovo L470\Desktop\2phGWO\Untitled.m*
Untitled.m* x Untitled2.m x Untitled3* x +
1 - clc;clear all;close all;
2 - %Two -phase Hybrid Stepping Motor
3 - X=[2750000 28350000 135000000];
4 - Y=[1 19799 650000 7500 0];
5 - G=tf(X,Y)
6 - step(G)
7
Command Window
G =
2.75e06 s^2 + 2.835e07 s + 1.35e08
-----
s^4 + 19799 s^3 + 650000 s^2 + 7500 s
Continuous-time transfer function.
    
```

a. The modeling by m-file



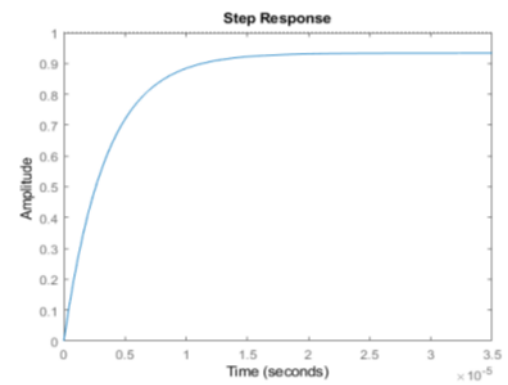
b. The results by m-file

Fig. 23. Open loop system

```

Editor - C:\Users\Lenovo L470\Desktop\2phGWO\Untitled2.m*
Untitled.m x Untitled2.m* x Untitled3* x +
1 - clc;clear all;close all;
2 - %Two -phase Hybrid Stepping Motor
3 - X=[2750000 28350000 135000000];
4 - Y=[1 19799 650000 7500 0];
5 - G=tf(X,Y)
6 - Gf=feedback(G,1);
7 - step(Gf)
8
Command Window
G =
2.75e06 s^2 + 2.835e07 s + 1.35e08
-----
s^4 + 19799 s^3 + 650000 s^2 + 7500 s
Continuous-time transfer function.
    
```

a. The modeling by m-file



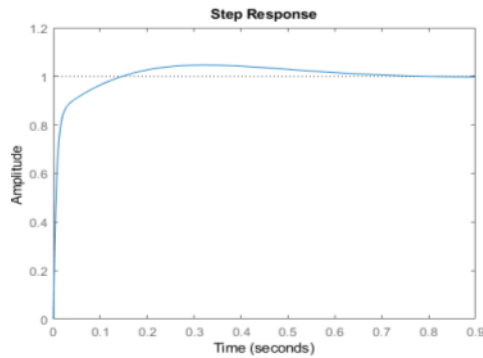
b. The results by m-file

Fig. 24. Close loop system

```

Editor - C:\Users\Lenovo L470\Desktop\2phGWO\Untitled3.m
1  Untitled.m  Untitled2.m  Untitled3.m  +
1  clc;clear all;close all;
2  %Two -phase Hybrid Stepping Motor
3  X=[2750000 28350000 135000000];
4  Y=[1 19799 650000 7500 0];
5  G=tf(X,Y)
6  Gf=feedback(G,1);
7  kp=10;
8  ki=1;
9  kd=0.1;
10 Gc=pid(kp,ki,kd);
11 Gcf=feedback(Gc*G,1);
12 step(Gcf)
13
Command Window
G =
      2.75e06 s^2 + 2.835e07 s + 1.35e08
-----
      s^4 + 19799 s^3 + 650000 s^2 + 7500 s
Continuous-time transfer function.
    
```

a. The modeling by m-file



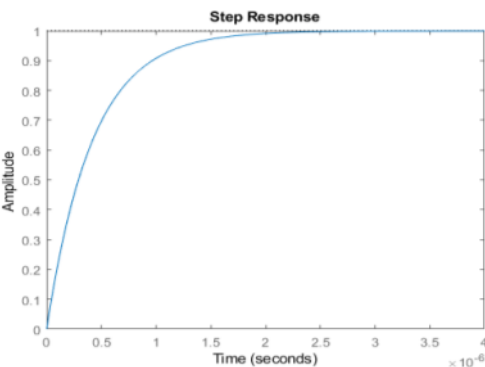
b. The results by m-file

Fig. 25. Close loop system with PID controller

```

Editor - E:\2phGWO\Untitled12345.m
1  Untitled12345.m  +
1  clc;clear all;close all;
2  %Two -phase Hybrid Stepping Motor
3  X=[2750000 28350000 135000000];
4  Y=[1 19799 650000 7500 0];
5  G=tf(X,Y)
6  Gf=feedback(G,1);
7  %GWO
8  iter=50;
9  pop=20;
10 a_gwo=2;
11 Var=3;
12 %Search Space
13 al=0;%Lower bound
14 au=500;%Upper bound
15 c_cf=0;
16 %initialization
17 for p=1:pop
18
19     for n=1:Var
20         x(p,n)=al+rand*(au-al);
21     end
    
```

a. The modeling by m-file



b. The results by m-file

Fig. 26. Close loop system with PID controller

IV. CONCLUSION

Simulation and engine model building were performed using MATLAB (SIMULINK) software. Specifications were chosen to fit the proposed application to run a motor in a robotic system for surface grinding process, such as a turbine fan or a steamer. The effectiveness of the model and the validity of the system were also verified. The possibility of improving the performance of the motor with different working conditions similar to real-time operation was verified. The aim of the research is to simulate a working system of a robot that is managed and moved by the proposed electric motor of the two-phase hybrid stepper motor by adopting the use of the computer and building the model from the MATLAB program package to perform the grinding process and control the force as a result of the surface difference during the grinding process. The advantage and clear superiority of the smart system over the traditional one, and the control using a traditional unit is also effective in the process of improving performance with the system.

REFERENCES

- [1] Q. Ariyansyah and A. Ma'arif, "DC Motor Speed Control with Proportional Integral Derivative (PID) Control on the Prototype of a Mini-Submarine," *JFSC*, vol. 1, no. 1, pp. 18–24, 2023, <https://doi.org/10.59247/jfsc.v1i1.26>.
- [2] A. J. Attiya, Y. Wenyu, S. W. Shneen "PSO_PI controller of robotic grinding force servo system," *TELKOMNIKA Indonesian Journal of Electrical Engineering*, vol. 15, no. 3, pp. 515-525, 2015, <http://doi.org/10.11591/tjee.v15i3.1570>.
- [3] M. Alfian and R. D. Puriyanto, "Mecanum 4 Omni Wheel Directional Robot Design System Using PID Method," *JFSC*, vol. 1, no. 1, pp. 6–13, 2023, <https://doi.org/10.59247/jfsc.v1i1.27>.
- [4] A. J. Attiya, S. W. Shneen, B. A. Abbas, Y. Wenyu, "Variable speed control using fuzzy-pid controller for two-phase hybrid stepping motor in robotic grinding," *Indonesian Journal of Electrical Engineering and Computer Science*, vol. 3, no. 1, pp. 102-118, 2016, <https://doi.org/10.11591/ijeecs.v3.i1.pp102-118>.
- [5] A. J. Attiya, Y. Wenyu, S. W. Shneen, "Compared with PI, Fuzzy-PI and PSO-PI controllers of robotic grinding force servo system," *TELKOMNIKA Indonesian Journal of Electrical Engineering*, vol. 16, no. 1, pp. 65-74, 2015, <https://doi.org/10.11591/tjee.v16i1.1589>.
- [6] A. J. Attiya, Y. Wenyu, S. W. Shneen, "Fuzzy-PID controller of robotic grinding force servo system," *TELKOMNIKA Indonesian Journal of Electrical Engineering*, vol. 15, no. 1, pp. 87-99, 2015, <https://doi.org/10.11591/telkomnika.v15i1.8051>.
- [7] H. Maghfiroh, J. Slamet Saputro, F. Fahmizal, and M. Ahmad Baballe, "Adaptive Fuzzy-PI for Induction Motor Speed Control," *JFSC*, vol. 1, no. 1, pp. 1–5, 2023, <https://doi.org/10.59247/jfsc.v1i1.24>.
- [8] Fahmizal, D. Yanu Kharisma, and S. Pramono, "Implementation of Fuzzy Logic Control on a Tower Copter," *JFSC*, vol. 1, no. 1, pp. 14–17, 2023, <https://doi.org/10.59247/jfsc.v1i1.25>.
- [9] M. A. Al-bahrany and A. T. A. Sada, "Smart Dc to Dc converter for a Small Drone Based upon Deep Learning Technique," *JFSC*, vol. 1, no. 2, pp. 55–60, 2023, <https://doi.org/10.59247/jfsc.v1i2.43>.
- [10] H. Maghfiroh, C. Hermanu, M. H. Ibrahim, M. Anwar, A. Ramelan, "Hybrid fuzzy-PID like optimal control to reduce energy consumption," *TELKOMNIKA (Telecommunication Computing Electronics and Control)*, vol. 18, no. 4, pp. 2053-2061, 2020, <http://doi.org/10.12928/telkomnika.v18i4.14535>.
- [11] H. S. Dakheel, Z. B. Abdullah, N. S. Jasim, S. W. Shneen, "Simulation model of ANN and PID controller for direct current servo motor by using Matlab/Simulink," *TELKOMNIKA (Telecommunication Computing Electronics and Control)*, vol. 20, no. 4, pp. 922-932, 2022, <http://doi.org/10.12928/telkomnika.v20i4.23248>.
- [12] S. W. Shneen, H. S. Dakheel, Z. B. Abdullah, "Design and Implementation of No Load, Constant and Variable Load for DC Servo

- Motor." *Journal of Robotics and Control (JRC)*, vol. 4, no. 3, pp. 323-329, 2023, <https://doi.org/10.18196/jrc.v4i3.17387>.
- [13] H. Maghfiroh, I. Iftadi, A. Sujono, "Speed control of induction motor using LQG," *Journal of Robotics and Control (JRC)*, vol. 2, no. 6, pp. 565-570, 2021, <https://doi.org/10.18196/26138>.
- [14] H. Maghfiroh, M. Nizam, M. Anwar and A. Ma'arif, "Improved LQR Control Using PSO Optimization and Kalman Filter Estimator," *IEEE Access*, vol. 10, pp. 18330-18337, 2022, <https://doi.org/10.1109/ACCESS.2022.3149951>.
- [15] H. Maghfiroh, A. Ma'arif, F. Adriyanto, I. Suwarno, W. Caesarendra, "Adaptive Linear Quadratic Gaussian Speed Control of Induction Motor Using Fuzzy Logic," *Journal Européen des Systèmes Automatisés*, vol. 56, no. 4, pp. 703-711, 2023, <https://doi.org/10.18280/jesa.560420>.
- [16] H. S. Dakheel, Z. B. Abdullah, N. S. Jasim, S. W. Shneen, "Simulation model of ANN and PID controller for direct current servo motor by using Matlab/Simulink," *TELKOMNIKA (Telecommunication Computing Electronics and Control)*, vol. 20, no. 4, pp. 922-932, 2022, <http://doi.org/10.12928/telkomnika.v20i4.23248>.
- [17] S. Waley, C. Mao, N. K. Bachache, "Biogeography based optimization tuned fuzzy logic controller to adjust speed of electric vehicle," *TELKOMNIKA Indonesian Journal of Electrical Engineering*, vol. 16, no. 3, pp. 509-519, 2015, <http://doi.org/10.11591/tjee.v16i3.1642>.
- [18] A. Batool, N. U. Ain, A. A. Amin, M. Adnan, M. H. Shahbaz, "A comparative study of DC servo motor parameter estimation using various techniques," *Automatika*, vol. 63, no. 2, pp. 303-312, 2022, <https://doi.org/10.1080/00051144.2022.2036935>.
- [19] D. Saputra, A. Ma'arif, H. Maghfiroh, P. Chotikunanan, S. N. Rahmadhia, "Design and Application of PLC-based Speed Control for DC Motor Using PID with Identification System and MATLAB Tuner," *International Journal of Robotics and Control Systems*, vol. 3, no. 2, pp. 233-244, 2023, <https://doi.org/10.31763/ijrcs.v3i2.775>.
- [20] A. Ma'arif, I. Suwarno, H. Maghfiroh, W. Rahmiani, A. A. Nuryono and N. M. Raharja, "Sliding Mode Control of Angular Speed DC Motor System with Parameter Uncertainty," *2022 IEEE International Conference on Communication, Networks and Satellite (COMNETSAT)*, pp. 380-387, 2022, <https://doi.org/10.1109/COMNETSAT56033.2022.9994286>.
- [21] A. Ma'arif, N. R. Setiawan, "Control of DC motor using integral state feedback and comparison with PID: simulation and arduino implementation," *Journal of Robotics and Control (JRC)*, vol. 2, no. 5, pp. 456-461, 2021, <https://doi.org/10.18196/jrc.25122>.
- [22] P. Ramesh Babu and V. Prabhu, "Modeling and performance analysis of Buck Converter fed PBLDC Motor Drives in Matlab/Simulink environment," *2013 International Conference on Circuits, Power and Computing Technologies (ICCPCT)*, pp. 219-224, 2013, <https://doi.org/10.1109/ICCPCT.2013.6529014>.
- [23] R. Kristiyono, Wiyono, "Autotuning Fuzzy PID Controller for Speed Control of BLDC Motor," *Journal of Robotics and Control (JRC)*, vol. 2, no. 5, pp. 400-407, 2021, <https://doi.org/10.18196/jrc.25114>.
- [24] S. W. Shneen, H. S. Dakheel, Z. B. Abdulla, "Advanced Optimal for PV system coupled with PMSM," *Indonesian Journal of Electrical Engineering and Computer Science*, vol. 1, no. 3, pp. 556-565, 2016, <https://doi.org/10.11591/ijeecs.v1.i3.pp556-565>.
- [25] A. Muttaqin, S. D. Finnadi, Z. Abidin, K. Araki, "FPGA based synchronous multi-channel PWM generator for humanoid robot," *International Journal of Electrical & Computer Engineering*, vol. 11, no. 1, pp. 2088-8708, 2021, <http://doi.org/10.11591/ijece.v11i1.pp249-256>.
- [26] A. S. Ahmed, H. A. Marzog, L. A. A. Rahaim, "Design and implement of robotic arm and control of moving via IoT with Arduino ESP32," *International Journal of Electrical & Computer Engineering*, vol. 11, no. 5, pp. 2088-8708, 2021, <http://doi.org/10.11591/ijece.v11i5.pp3924-3933>.
- [27] S. W. Shneen, G. A. Aziz, "Simulation model of 3-phase PWM rectifier by using MATLAB/Simulink," *International Journal of Electrical and Computer Engineering*, vol. 11, no. 5, p. 3736, 2021, <http://doi.org/10.11591/ijece.v11i5.pp3736-3746>.
- [28] D. H. Shaker, S. W. Shneen, F. N. Abdullah, G. A. Aziz, "Simulation Model of Single-Phase AC-AC Converter by Using MATLAB," *Journal of Robotics and Control (JRC)*, vol. 3, no. 5, pp. 656-665, 2022, <https://doi.org/10.18196/jrc.v3i5.15213>.
- [29] N. Salem, K. Mateen, W. Alharbi and J. Kamal, "Performance of LQR and PID Controllers for RS-550VC Motor Speed Enhancement," *2023 6th International Conference on Intelligent Robotics and Control Engineering (IRCE)*, pp. 01-06, 2023, <https://doi.org/10.1109/IRCE59430.2023.10255039>.
- [30] A. L. Shurajji, S. W. Shneen, "Fuzzy Logic Control and PID Controller for Brushless Permanent Magnetic Direct Current Motor: A Comparative Study," *Journal of Robotics and Control (JRC)*, vol. 3, no. 6, pp. 762-768, 2022, <https://doi.org/10.18196/jrc.v3i6.15974>.
- [31] J. A. Mohammed, A. L. Shurajji, "Modeling of DC elevator motor drive for mid-rise building," *Engineering & Technology Journal*, vol. 31, no. 12, pp. 2320-2342, 2013, <https://doi.org/10.30684/etj.31.12A.10>.
- [32] G. A. Aziz, S. W. Shneen, F. N. Abdullah, D. H. Shaker, "Advanced optimal GWO-PID controller for DC motor," *Int. J. Adv. Appl. Sci.*, vol. 11, no. 3, pp. 263-276, 2022, <http://doi.org/10.11591/ijaas.v11.i3.pp263-276>.
- [33] Y. Zhu, X. He, Q. Liu, W. Guo, "Semiclosed-loop motion control with robust weld bead tracking for a spiral seam weld beads grinding robot," *Robotics and Computer-Integrated Manufacturing*, vol. 73, p. 102254, 2022, <https://doi.org/10.1016/j.rcim.2021.102254>.
- [34] H. Maghfiroh, M. Ahmad, A. Ramelan, F. Adriyanto, "Fuzzy-PID in BLDC Motor Speed Control Using MATLAB/Simulink," *Journal of Robotics and Control (JRC)*, vol. 3, no. 1, pp. 8-13, 2022, <https://doi.org/10.18196/jrc.v3i1.10964>.
- [35] S. W. Jeab, A. Z. Salman, Q. A. Jawad, H. Shareef, "Advanced optimal by PSO-PI for DC motor," *Indonesian Journal of Electrical Engineering and Computer Science*, vol. 16, no. 1, pp. 165-175, 2019, <http://doi.org/10.11591/ijeecs.v16i1.pp165-175>.
- [36] A. Latif, A. Z. Arfianto, H. A. Widodo, R. Rahim, E. T. Helmy, "Motor DC PID system regulator for mini conveyor drive based-on MATLAB," *Journal of Robotics and Control (JRC)*, vol. 1, no. 6, pp. 185-190, 2020, <https://doi.org/10.18196/jrc.1636>.
- [37] H. J. Pahk, D. S. Lee, J. H. Park, "Ultra precision positioning system for servo motor-piezo actuator using the dual servo loop and digital filter implementation," *International Journal of Machine Tools and Manufacture*, vol. 41, no. 1, pp. 51-63, 2001, [https://doi.org/10.1016/S0890-6955\(00\)00061-4](https://doi.org/10.1016/S0890-6955(00)00061-4).
- [38] M. L. Zegai, M. Bendjebbar, K. Belhadri, M. L. Doumbia, B. Hamane and P. M. Koumba, "Direct torque control of Induction Motor based on artificial neural networks speed control using MRAS and neural PID controller," *2015 IEEE Electrical Power and Energy Conference (EPEC)*, pp. 320-325, 2015, <https://doi.org/10.1109/EPEC.2015.7379970>.
- [39] Z. B. Abdullah, S. W. Shneen, H. S. Dakheel, "Simulation Model of PID Controller for DC Servo Motor at Variable and Constant Speed by Using MATLAB," *Journal of Robotics and Control (JRC)*, vol. 4, no. 1, pp. 54-59, 2023, <https://doi.org/10.18196/jrc.v4i1.15866>.
- [40] G. Boukhalfa, S. Belkacem, A. Chikhi, S. Benagougne, "Direct torque control of dual star induction motor using a fuzzy-PSO hybrid approach," *Applied Computing and Informatics*, vol. 18, no. 1/2, pp. 74-89, 2020, <https://doi.org/10.1016/j.aci.2018.09.001>.
- [41] A. R. Ajel, H. M. A. Abbas, M. J. Mnati, "Position and speed optimization of servo motor control through FPGA," *International Journal of Electrical & Computer Engineering*, vol. 11, no. 1, pp. 2088-8708, 2021, <http://doi.org/10.11591/ijece.v11i1.pp319-327>.
- [42] A. N. Abdullah, M. H. Ali, "Direct torque control of IM using PID controller," *International Journal of Electrical and Computer Engineering*, vol. 10, no. 1, p. 617, 2020, <http://doi.org/10.11591/ijece.v10i1.pp617-625>.
- [43] H. S. Dakheel, Z. B. Abdullah, S. W. Shneen, "Advanced optimal GA-PID controller for BLDC motor," *Bulletin of Electrical Engineering and Informatics*, vol. 12, no. 4, pp. 2077-2086, 2023, <https://doi.org/10.11591/eei.v12i4.4649>.
- [44] B. B. Acharya, S. Dhakal, A. Bhattarai, N. Bhattarai, "PID speed control of DC motor using meta-heuristic algorithms," *International Journal of Power Electronics and Drive Systems*, vol. 12, no. 2, p. 822, 2021, <http://doi.org/10.11591/ijpeds.v12i2.pp822-831>.
- [45] F. N. Abdullah, G. A. Aziz, S. W. Shneen, "Simulation Model of Servo Motor by Using Matlab," *Journal of Robotics and Control (JRC)*,

- vol. 3, no. 2, pp. 176-179, 2022, <https://doi.org/10.18196/jrc.v3i2.13959>.
- [46] S. Usha, P. M. Dubey, R. Ramya, M. V. Suganyadevi, "Performance enhancement of BLDC motor using PID controller," *International Journal of Power Electronics and Drive Systems*, vol. 12, no. 3, 2021, <https://doi.org/10.11591/ijpeds.v12.i3.pp1335-1344>.
- [47] G. Boukhalfa, S. Belkacem, A. Chikhi, S. Benagoune, "Genetic algorithm and particle swarm optimization tuned fuzzy PID controller on direct torque control of dual star induction motor," *Journal of Central South University*, vol. 26, no. 7, pp. 1886-1896, 2019, <https://doi.org/10.1007/s11771-019-4142-3>.
- [48] S. W. Shneen, D. H. Shaker, F. N. Abdullah, "Simulation model of PID for DC-DC converter by using MATLAB," *International Journal of Electrical and Computer Engineering*, vol. 11, no. 5, p. 3791, 2021, <https://doi.org/10.11591/ijece.v11i5.pp3791-3797>.
- [49] S. W. Shneen, F. N. Abdullah, D. H. Shaker, "Simulation on model of single phase PWM inverter by using MATLAB/Simulink," *International Journal of Power Electronics and Drive Systems*, vol. 12, no. 1, p. 212, 2021, <http://doi.org/10.11591/ijpeds.v12.i1.pp212-216>.
- [50] S. W. Shneen, H. S. Dakheel, Z. B. Abdulla, "Design and implementation of variable and constant load for induction motor," *International Journal of Power Electronics and Drive Systems*, vol. 11, no. 2, p. 762, 2020, <http://doi.org/10.11591/ijpeds.v11.i2.pp762-773>.